

LTESS-track: A Precise and Fast Frequency Offset Estimation for low-cost SDR Platforms

Roberto Calvo-Palomino

IMDEA Networks Institute, Madrid, Spain &
Universidad Carlos III de Madrid, Spain
roberto.calvo@imdea.org

Domenico Giustiniano

IMDEA Networks Institute, Madrid, Spain
domenico.giustiniano@imdea.org

ABSTRACT

The availability of very cheap RTL-SDR "dongle" devices has unleashed the popularity of Software-Defined Radio (SDR) projects in the last years, both among academics and hobbyists. The main success factors are the very affordable price (< 25 USD), ease of use and wide availability of open-source SDR software. One important performance aspect of SDR receivers is related to the accuracy and stability of the Local Oscillator (LO). We present LTESS-track, an LO frequency offset evaluation method that relies on the Synchronization Signals (SS) transmitted by LTE base stations as reference. We compare LTESS-track with other publicly available tools for frequency offset estimation and show that our method can perform reliable measurements in less than 1 second, orders of magnitude faster than software publicly available. We leverage LTESS-track to assess the actual LO performances of two popular RTL-SDR models with and without Temperature Controlled Local Oscillator (TCXO). The experimental results show that the latest generation of RTL-SDR (with TCXO), despite being very low cost, has surprising excellent LO stability, well within the maximum tolerance of 1 ppm declared in the specifications.

KEYWORDS

frequency offset estimator; LTE; rtl-sdr; open source

1 INTRODUCTION

The field of Software-Defined Radio (SDR) is becoming increasingly popular among academics and practitioners. The popularity of SDR was unleashed by the combined availability of low-cost SDR hardware and free open-source SDR software. The so-called RTL-SDR dongle devices are nowadays among the most popular in the SDR community and are largely used in crowd-sourced projects such as Electrosense [9], OpenSky [12] and others [6].

Permission to make digital or hard copies of all or part of this work for personal or classroom use is granted without fee provided that copies are not made or distributed for profit or commercial advantage and that copies bear this notice and the full citation on the first page. Copyrights for components of this work owned by others than ACM must be honored. Abstracting with credit is permitted. To copy otherwise, or republish, to post on servers or to redistribute to lists, requires prior specific permission and/or a fee. Request permissions from permissions@acm.org.

WiNTECH'17, October 20, 2017, Snowbird, UT, USA

© 2017 Association for Computing Machinery.

ACM ISBN 978-1-4503-5147-8/17/10...\$15.00

<https://doi.org/10.1145/3131473.3131481>

Fabio Ricciato

University of Ljubljana, Slovenia
fabio.ricciato@fri.uni-lj.si

Vincent Lenders

armasuisse, Thun, Switzerland
vincent.lenders@armasuisse.ch

Generally speaking, low-cost devices may be expected to have much higher LO instability than other classical receivers, possibly limiting some potential applications. For example, in advanced decoding schemes based on interference cancellation (in space and/or time) decoders may need to compensate for frequency offset effects during the duration of a single packet. A time-varying LO offset might impede the correct estimation of time-of-arrival or time-difference-of-arrival, as relevant e.g. in time-based localization, since timing information is ultimately derived from LO. Also, it might impede the correct estimation of Doppler shifts [10]. In all such application categories, the software designer should then decide whether to include more or less sophisticated frequency correction methods into the SDR code to counteract the LO frequency deviations and fluctuations.

In general, understanding LO offset near real-time is essential to take the most appropriate actions. Low measurement delay is important for two reasons. First, it allows to swiftly evaluate short-term frequency fluctuations of the device under test using a recorded dataset. Second, it can be used as an ancillary tool serving other SDR applications that requires periodic re-estimation of absolute LO offset. For instance, low-cost RTL-SDR sensors scanning the spectrum may periodically re-tune their center frequency to some common LTE base station in order to estimate and correct their LO offset. This procedure should be as fast as possible to minimize any outage in the measurement campaign.

The contribution of this work are three-fold:

- We present LTESS-track, a LO frequency offset evaluation tool that allows SDR practitioners to determine the frequency offset of their SDR devices without the need to acquire additional laboratory equipment, such as high-end signal generators or other methods. LTESS-track leverages the ubiquity of LTE (Long Term Evolution) coverage: it exploits the Primary Synchronization Signal (PSS) that is continuously broadcast by LTE base stations as a reference signal of opportunity. In principle, LTESS-track can work with any SDR front-end capable of tuning to LTE frequencies. Our method is designed to deliver a frequency offset estimation with sub-ppm resolution and *maximum measurement delay below 1 second*. This is a particular feature of LTESS-track, not present in other existing LO offset estimation methods [1–3].
- We compare LTESS-track against three other popular software methods for low-cost LO offset estimation, namely the *rtl_test* [3], Kalibrate-RTL [1] and LTE-Cell-Scanner [2]. We

show that previous works have under-exploited the potential of cellular signaling for frequency offset estimation and we demonstrate that our architecture design allows to achieve higher performance. As we show in our work, one common limitation of previous methods is the high measurement delay, up to 12 seconds (Kalibrate-RTL) or even several minutes (rtl_test). Furthermore, we show that some of these other tools present occasionally large errors (LTE-Cell-Scanner), or simply do not work in the presence of large LO offset (Kalibrate-RTL).

- We use our method to assess the actual LO performance of two very popular RTL-SDR models, namely the "Silver" and "Blue" models, respectively with and without Temperature Controlled Local Oscillator (TCXO). We consider both normal and harsh environments, with device temperatures exceeding 50 degrees Celsius. The results show how the new generation of RTL-SDR with TCXO, despite its low cost, has an exceptional LO stability in changing temperature environments.

LTESS-track implements several key mechanisms not presented in other methods, such as initial frequency offset compensation, upsampling, sampling of data only in time proximity to the expected synchronization signal to reduce the computational cost and linear regression of samples. Our method will further contribute to the "popularization" of low-cost SDR development and related crowd-sourced SDR projects.

2 PROBLEM STATEMENT

2.1 Receiver model

The available specifications do not provide the exact details in all the levels of the RTL-SDR hardware architecture [4]. For our work we have assumed the general architecture depicted in Fig. 1 with a single Local Oscillator (LO) that feeds both the Down-Conversion (DC) and the Sampling (S) stage by means of two distinct clock distribution networks.

We introduce the following notation:

- f_{LO} the *nominal* LO frequency.
- $\Delta f_{LO}(t)$ the difference between the *actual* LO frequency at time t and its nominal value, i.e., the *absolute* frequency offset of LO.
- $\gamma(t) \stackrel{\text{def}}{=} \frac{\Delta f_{LO}}{f_{LO}}$ the instantaneous *relative* frequency offset of LO at time t .
- f_D the *nominal* tune-in frequency.
- $\Delta f_D(t)$ the difference between the *actual* and nominal tune-in frequency at time t , i.e., the *absolute* frequency offset at the down-conversion stage.
- f_S the *nominal* sampling rate.
- $\Delta f_S(t)$ the difference between the *actual* and nominal sampling rate at time t , i.e., the *absolute* frequency offset at the sampling stage.

In general, we can assume that the *relative* frequency offset at the down-conversion and sampling stage are equal or anyway very close to the LO one, formally:

$$\frac{\Delta f_S(t)}{f_S} \approx \frac{\Delta f_D(t)}{f_D} \approx \frac{\Delta f_{LO}(t)}{f_{LO}} = \gamma(t). \quad (1)$$

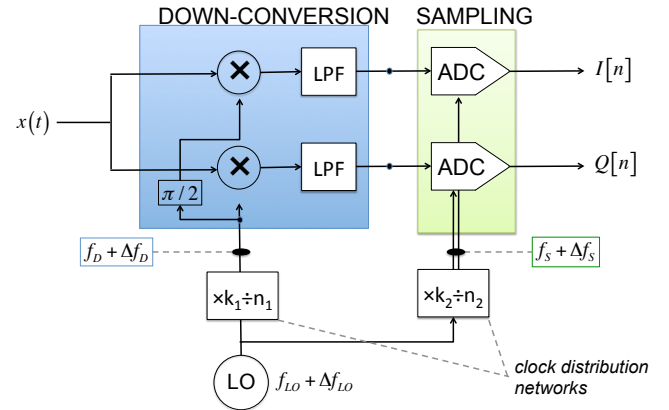


Figure 1: Reference receiver architecture.

The relative frequency offset $\gamma(t)$ is a dimension-less parameter. The specifications typically provide an indication of the maximum LO frequency tolerance ϕ expressed in parts-per-million (ppm). For example, a relative frequency tolerance of 30 ppm means a maximum time offset of 30 microseconds in one second. The tolerance value represents an upper bound on the maximum relative deviation that may be expected, i.e. $|\gamma(t)| \leq \phi$.

2.2 Design goals

Our goal is to develop a generic method to estimate and evaluate the frequency offset of the low-cost RTL-SDR devices with the following features:

- *Reliable*: The method should report a reliable estimate of the LO frequency offset, with estimation error below 1 ppm.
- *Fast*: The method should be fast to provide new estimates with a maximum delay of 1 second, in order to minimize any outage in the spectrum measurement campaign.
- *Flexible*: The method shall be flexible enough to work with different RTL-SDR devices (TCXO and non-TCXO models), possibly with large LO offset values (several tens of ppm).
- *Efficient*: The method should be executed in small-factor embedded architectures such as Raspberry Pi.

3 LTESS-track

In this section, we detail the proposed methodology to estimate the LO offset of SDR devices. Our method relies on the availability of LTE signals that are captured by the SDR devices.

3.1 LTE Signal model

We first briefly review a few fundamental concepts about LTE. Typically in LTE networks, the user needs to get the cell id of the base station and the frame synchronization to perform more complex operations. The first step in order to get the proper time and frequency synchronization is to search for the PSS (*Primary Synchronization Signal*) and SSS (*Second Synchronization Signal*) which have a band of 1.4 MHz [11, Chapter 7] [5]. LTE defines two structures called frame and subframe [11]. Each frame has a duration of 10 ms and contains 10 subframes of 1 ms each. The

Table 1: LTE Parameters

T_F	10 ms	Nominal period of LTE frames.
f_S	1.92 MHz	Nominal sampling frequency.
T_S	520 ns	Sampling period (f_S^{-1})
f_D	806 MHz	Nominal center frequency of the LTE cell *

* We have tested three different LTE cells at different frequencies: 796 MHz, 806 MHz and 816 MHz. All results were very similar. In this work we present only the results for the 806 MHz cell.

PSS and SSS signals can be found in subframes 0 and 5 of every frame. The PSS is a frequency-domain Zadoff-Chu [5] 128 bits long sequence and encodes the layer identity of the cell. The SSS encodes the cell identity and is modulated using binary phase-shift keying (BPSK). For our purposes, we consider only the PSS signal and its periodicity (twice every 10 ms) to design a frequency offset estimation method.

The choice of LTE synchronization signals as absolute clock reference is motivated by the very high precision and stability of such signals: in fact, LTE base stations must meet strict requirements in terms of frequency stability with maximum tolerance below 0.05 ppm [7], i.e., much smaller than the expected tolerance of RTL-SDR devices currently on the market.

We consider the LTE parameters as shown in Table 1. The input stream of complex baseband IQ samples at the sampling rate f_S will be denoted by $x[n] \stackrel{\text{def}}{=} x(t)|_{t=nT_s}$. We shall index in $k = 0, 1, \dots$ consecutive LTE frames. Without loss of generality, we fix the time origin at the (true) arrival time of the PSS signal for the first frame $k = 0$. For the generic k -th frame, we denote by $y[k]$ the true (unknown) PSS arrival time, and by $\hat{y}[k]$ the corresponding *measured* value, as obtained with the measurement procedure detailed later in Section 3.2. Two distinct sources of errors affect the measured value $\hat{y}[k]$: the clock error ρ_k and the measurement noise e_k , i.e.

$$\hat{y}[k] = y[k] + \rho_k + e_k = kT_F + \rho_k + e_k. \quad (2)$$

The measurement noise term e_k is modeled by a sequence of i.i.d. random variables with zero-mean and variance σ_e^2 . The clock error accumulated until the k -th frame is given by the integral of the instantaneous (relative) frequency deviation $\gamma(t)$ and can be developed as

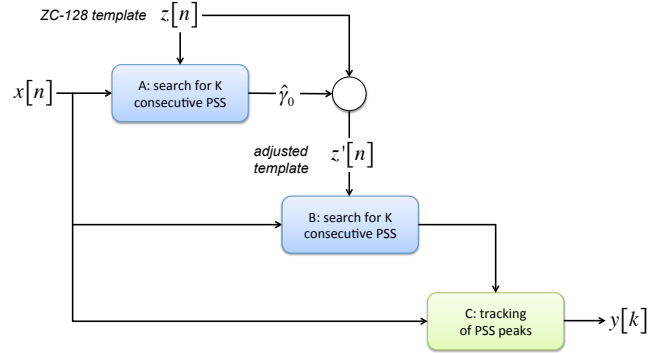
$$\rho_k = \int_0^{kT_F} \gamma(t) dt \approx \gamma kT_F + \int_0^{kT_F} \sum_{n=1}^{\ell} \beta_n t^n dt, \quad (3)$$

wherein the last term represents the time-varying component of the LO frequency and is modeled (approximated) by a polynomial of sufficiently high degree ℓ . From Eq. (3) we derive the general signal model for time-varying LO frequency:

$$\hat{y}[k] = (1 + \gamma) \cdot kT_F + \sum_{n=2}^{\ell+1} \alpha_n k^n + e_k \quad (4)$$

with $\alpha_n = \beta_n T_F^n / n$. For a short observation interval we can neglect the time-varying component ($\alpha_n = 0$, $n = 1, \dots, \ell$) and consider a *static* scenario with fixed frequency offset $\gamma(t) = \gamma$. In this special case the model simplifies as:

$$\hat{y}[k] = (1 + \gamma) \cdot kT_F + e_k. \quad (5)$$

**Figure 2: Overview of our PSS tracking algorithm.**

Consider an observation window of duration W seconds embedding $N \stackrel{\text{def}}{=} \lfloor \frac{W}{T_F} \rfloor$ frames. The vector of measurements collected in said window will be denoted by $\hat{y} \stackrel{\text{def}}{=} \{\hat{y}[k], k = 1, \dots, N\}$. The choice between the static model Eq. (5) and the dynamic model Eq. (4) depends on the duration W of the observation window and on the temporal stability of the LO. For short windows of a few seconds, we can neglect temporal variations and resort to the simpler static model Eq. (5).

3.2 Estimation of PSS arrival times

In this section, we describe the method implemented to obtain a precise estimate of the (sequence of) PSS arrival times $\hat{y}[k]$. The overall scheme is depicted in Fig. 2. The PSS tracking stage is preceded by an initial acquisition stage.

The core block of the PSS detection process is a correlation filter: a chunk of $L = 128$ samples from the input IQ stream starting at position m is correlated with the known ZC-128 template $z[n]$. However, we introduce the following refinements:

- Frequency offset compensation: in order to counteract the effect of frequency offset in the down-conversion stage, we consider the following frequency-adjusted template

$$z'[n] \stackrel{\text{def}}{=} z[n] \cdot \exp^{-j2\pi \hat{y}_0 \frac{f_D}{f_S}} \quad (6)$$

wherein \hat{y}_0 denotes a coarse initial estimate of the frequency offset, obtained during the initial acquisition phase.

- Up-sampling: in order to achieve sub-sample resolution for the individual estimate $\hat{y}[k]$ we up-sample the IQ stream by a large factor U . Unless differently specified we used $U = 40$. For more details on the principles of re-sampling and up-sampling refer to [8].
- To speed-up the computation process, in the tracking stage correlation and up-sampling are applied only to the portion of the incoming IQ stream in the neighborhood of the expected PSS position as predicted from the previous frame, and specifically in a search window of $\pm N_{\text{search}}$ samples centered at $\hat{y}[k-1] + T_F$, with $N_{\text{search}} \ll T_F f_S$.

Hereafter we elaborate on the need to consider the frequency-adjusted template Eq. (6). Generally speaking, for a continuous-time signal $s(t)$, the ambiguity function $A(\tau, v)$ is given by the cross-correlation of $s(t)$ with a copy of the same signal delayed in time

by τ (sec) and shifted in frequency by v (Hz), formally:

$$A(\tau, v) \stackrel{\text{def}}{=} \left| \int_{-\infty}^{\infty} s(t) \cdot s^*(t - \tau) \exp^{+j2\pi v t} dt \right| \quad (7)$$

In Fig. 3(a) we plot the ambiguity function for one of the ZC-128 sequences used for PSS. The horizontal lines in the plot correspond to frequency offset values that are relevant for our experiments, namely $v_1 = 0.8$ kHz and $v_2 = 53.2$ kHz. For a carrier frequency $f_D = 806$ MHz these values represent 1 ppm and 66 ppm CFO (carrier frequency offset), respectively. The corresponding sections of the ambiguity function in the delay domain are plotted in Fig. 3(b). From there, it is clear the effect that a large frequency offset (66 ppm) has onto the cross-correlation function: the single large peak at $\tau = 0$ vanishes while other secondary peaks get stronger, with the effect of shifting the "highest peak" position by several sample periods. It should be noted that such a pattern will anyway occur periodically – with apparent period γT_F at the receiver – due to the periodicity of the LTE frame structure. Since our goal is to estimate the actual *rate* of the PSS periodicity, and not the absolute *phase* of the periodic pattern, the delay shift introduced by a frequency offset at the down-conversion stage does not impede by itself the estimation process. However, the reduced strength of the highest peak is detrimental to the precision of the process. For this reason, we perform an initial estimation of the frequency offset using the original template $z[k]$ and then compensate for the frequency offset by considering the adjusted template $z'[k]$ defined in Eq. (6) instead of the original sequence $z[k]$ (c.f. Fig. 2).

3.3 Estimation of instantaneous frequency deviation

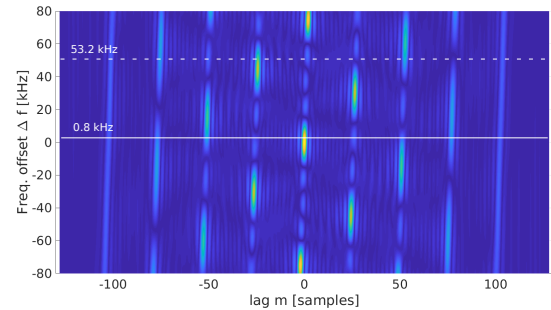
The overall estimation process is split into two stages:

- Estimation of PSS arrival times \hat{y} from the stream of IQ samples, as presented in the previous subsection.
- Estimation of the instantaneous frequency offset \hat{v} (or $\hat{v}(t)$ for the dynamic case) from the vector of PSS arrival times \hat{y} .

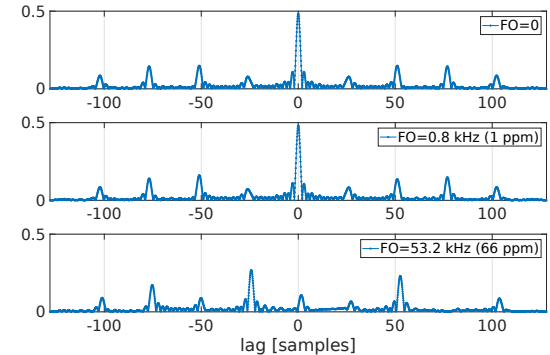
The latter is detailed in the present subsection.

If the observation window W is sufficiently short, we can neglect higher-order variations of the instantaneous LO frequency (i.e., frequency drift) occurring within the observation window and consider the fixed-frequency (static) model in Eq. (5). In this case, from the vector of N measurements $\hat{y}[k]$ we obtain an estimate \hat{v} simply by linear regression. The higher the precision of individual measurements (i.e., the lower σ_e), the faster a reliable estimate of \hat{v} can be achieved. In case of longer observation windows (larger W), we must consider the dynamic clock error model in Eq. (4). In this case, we apply higher-order polynomial regression in order to estimate the coefficients \hat{v} and $\hat{\alpha}_n$'s, and from the latter compute the $\hat{\beta}_n$'s. The collection of such parameters represents the full trajectory of the LO frequency within the (long) observation window.

To illustrate, in Fig. 4 we present the estimated profile of $\hat{v}(t)$ obtained with real devices during an observation window of 5 minutes. The continuous line was obtained by processing all the data from the whole long window of $W = 5$ minutes in a single batch, with regression to a high-order polynomial. The red circles represent the estimates obtained by splitting the dataset into short sub-windows of $W = 5$ seconds, with simple linear regression based on the static



(a) Ambiguity function in the Doppler/delay plane. The horizontal lines represent the sections plotted in Fig. 3(b).



(b) Autocorrelation sequences for the different frequency offset values (sections of ambiguity function).

Figure 3: Ambiguity function for one ZC-128 sequence.

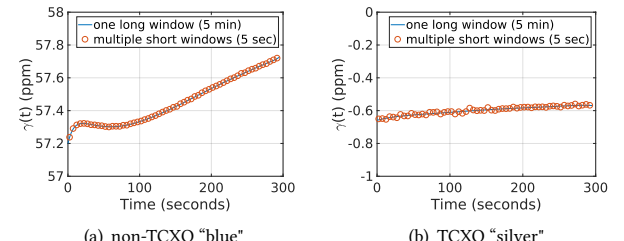


Figure 4: Short-term fluctuations: the red circles represent estimates obtained with short windows of 5 sec and linear regression. The continuous line represents the result of higher-order polynomial regression on the total window of 5 min.

model from Eq. (5). As expected, the two approaches lead to very similar estimates. Unless differently specified, in the remainder of this work we will adopt the short-window approach with linear regression in order to reduce complexity and computational time.



Figure 5: Hardware

4 EVALUATION

In this section, we detail the testbed used and explain the comparison made by LTESSTrack against three open source tools for frequency offset estimation.

4.1 Testbed

We deploy an outdoor testbed to perform the evaluation of the frequency offset for different RTL-SDR devices. We rely on the Raspberry-Pi (RBPi) as the main board (Fig. 5(a)) to execute the different tools in a Linux environment. We setup a set of RBPis in a small container with TCXO RTL-SDR devices (Fig. 5(b)) and non-TCXO RTL-SDR devices (Fig. 5(c)) attached to enable the comparison among the different frequency estimation methods. In addition to that, we also measure the ambient temperature and the temperature of the RTL-SDR case (with commercial temperature sensors) in order to study their relation with the frequency offset.

4.2 Evaluated tools

The following three existing tools have been considered for this study in addition to the newly proposed method:

- **rtl_test** [3]. This benchmark tool is part of the rtl-sdr software. The simple approach used for rtl_test is to count the samples read by the RTL-SDR device and compare it with the nominal sampling rate.
- **Kalibrate-RTL** [1]. This tool allows to scan and find GSM base stations in a frequency range and therefore use them to estimate the frequency offset of the rtl-sdr local oscillator.
- **LTE-Cell-Scanner** [2]. This tool performs a LTE base station search in a given frequency range. Once the base station is detected the tool reports the cell id and the frequency offset set estimated using the PSS and SSS defined in LTE structure [11, Chapter 7] [5].

We evaluate each tool described above against our LTESSTrack. As it is detailed below, we found some common limitations among those tools in terms of coarse time granularity, long processing time and, in some cases, gross estimation errors.

Comparison with rtl_test. The main limitation of the rtl_test tool is the coarse temporal resolution. This tool computes the frequency offset based on the difference between the actual number of IQ samples collected in each time-bin of duration ω interval $[0, \omega]$ and the expected number thereof based on the nominal sampling frequency. This method is affected by errors in the determination

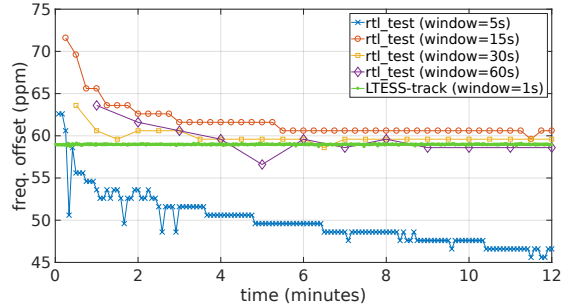


Figure 6: Comparison with rtl_test (non-TCXO).

of the reference interval ω in the absence of an accurate reference clock. rtl_test introduces a new source of error which is the frequency offset of the internal clock of the computer where the measurement is performed. In order to mitigate this error, two possible approaches can be taken: (1) choose a large value for W , and (2) average k subsequent measurements. The temporal resolution of the measurements is therefore $\tau \stackrel{\text{def}}{=} k \cdot \omega$. Fig. 6 shows the estimated LO frequency offset values reported by rtl_test after τ seconds based on the average of k subsequent measurements in window of size W , for different values of the latter. The measurement obtained with our method is also plotted as reference. It can be seen that even with the most favorable setting ($W = 60$ sec), it takes more than 3 minutes for rtl_test to approach the LO offset value as determined by LTESSTrack after 1 sec. Furthermore, with $W = 5$ sec the output values appear to be diverging. We conclude that rtl_test cannot be used to evaluate frequency offset variations at timescales smaller than a few minutes.

Comparison with Kalibrate-RTL. We observed that this tool delivers grossly erroneous results when used with devices affected by large frequency offsets. For example, for the “blue” non-TCXO dongle, it was reporting an estimated value of $\hat{\gamma} = -22$ ppm while all other tools were consistently reporting values around $\hat{\gamma} = +59$ ppm. The inaccuracy of this tool when applied on devices with LO offsets in excess of about 20 ppm is a known issue¹. The problem can be mitigated by providing a good initial guess of the LO frequency offset as input to the tool. That means Kalibrate-RTL can be used only to refine the initial estimate obtained by other means. In Fig. 7, we report the estimated values obtained with Kalibrate-RTL for different initial guess values given as input. It should be noted that even with proper initialization, the reported output value is sensitive to the exact input value.

Comparison with LTE-Cell-Scanner. Next, we tested LTE-Cell-Scanner. Similarly to our new tool, also LTE-cell-track relies on LTE signals as reference. This tool uses a fixed observation window of 160 ms and this is the value that we used in our tests. For most of the measurement timebins, the reported value were very close to the one estimated by our method—a clear indication of the precision of both tools. However, in less than 1% of the timebins we observed occasional large errors (see Fig. 9(a) and Fig. 9(b)). Another limitation of this tool is the heavy computation: on a RPi-3 it takes approximately 1 minute to process the data and report a frequency

¹<https://github.com/steve-m/kalibrate-rtl/issues/8>

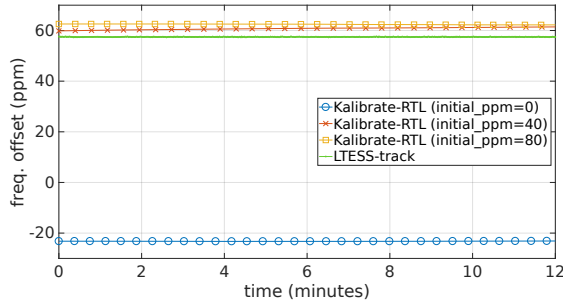
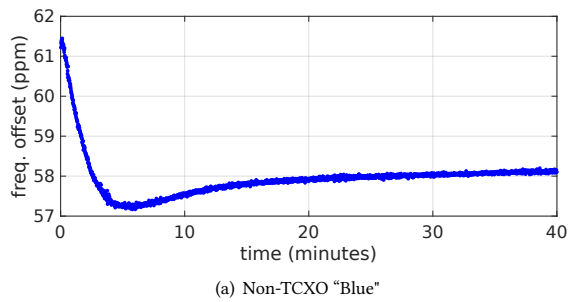
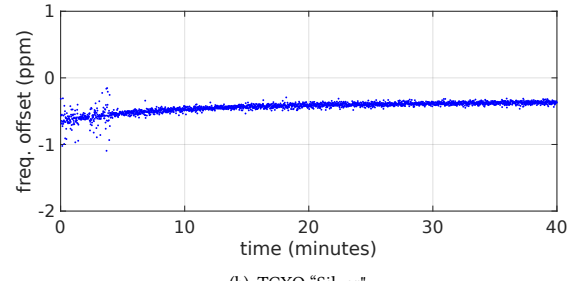


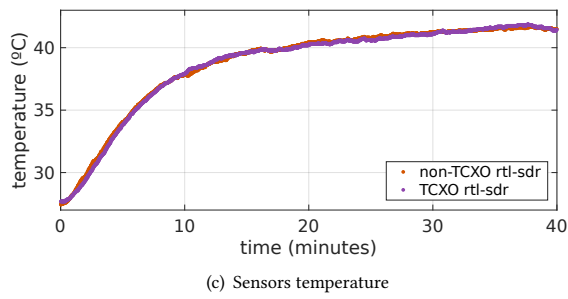
Figure 7: Comparison with Kalibrate-RTL (non-TCXO).



(a) Non-TCXO "Blue"



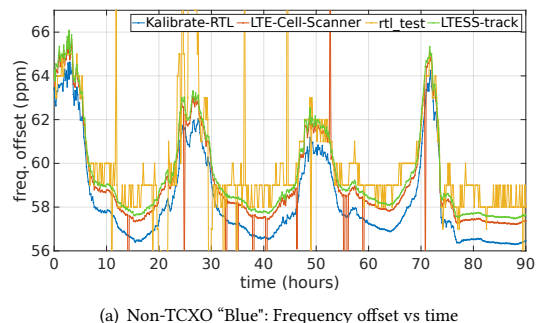
(b) TCXO "Silver"



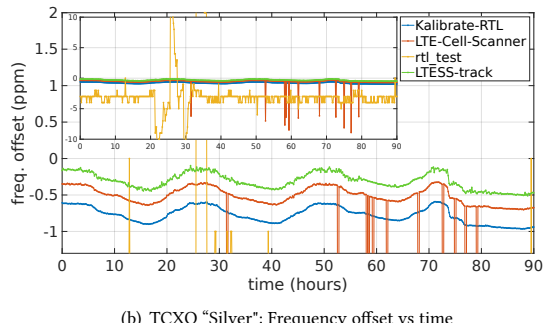
(c) Sensors temperature

Figure 8: Short-term frequency offset variations for Non-TCXO (top) and TCXO (middle) RTL-SDR devices. Sensors temperature is shown on the bottom.

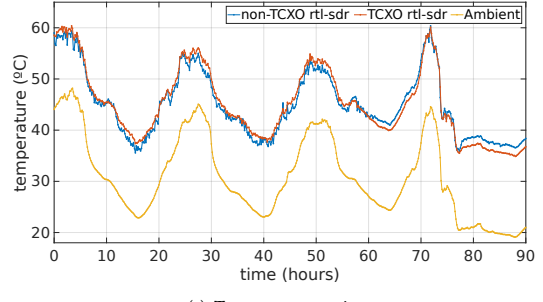
offset estimation. Due to such limitations, it is not possible with this tool to observe frequency offset fluctuations at small timescales.



(a) Non-TCXO "Blue": Frequency offset vs time



(b) TCXO "Silver": Frequency offset vs time



(c) Temperature vs time

Figure 9: Long-term frequency offset analysis.

4.3 Short-term variations

In Fig. 8(a) and Fig. 8(b), we plot the evolution of the LO frequency offset estimated with LTESSTrack. We run our method during the first 40 minutes of operation (starting from a cold state of the devices), respectively, for the blue and silver dongles. Fig. 8(c) shows the device temperature. An initial transitory state is clearly in place, with steeper LO frequency excursion due to initial heating. After approximately 20 min the device temperature stabilizes (around 40°C) and so does the LO frequency. For the non-TCXO dongle, we observe a maximum excursion of 4 ppm within the first 5 minutes. For the TCXO device, we observe a smaller variation of 0.8 ppm during the first 5 minutes. After this initial warm-up, the LO offset excursion remains contained within 0.2 ppm, well within the declared specifications of 1 ppm [4].

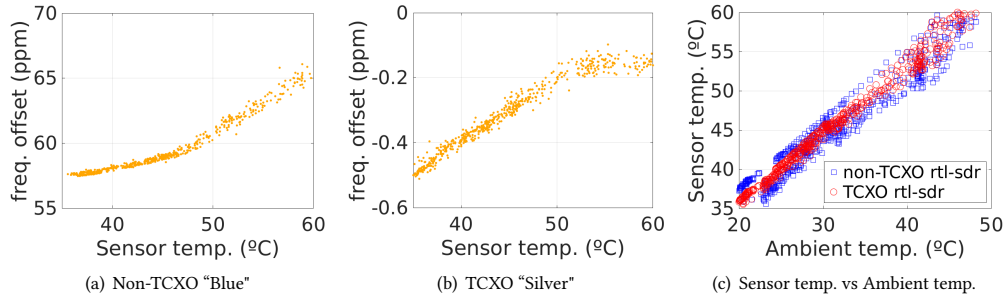


Figure 10: Frequency offset and temperature analysis.

4.4 Long-term variations

We have conducted a set of long-term measurements to evaluate LO offset variations of the RTL-SDR devices over a long period and across different temperatures, and at the same time to perform a long-term comparison of the output of different tools. The different tools were run on the same device in a round-robin fashion, with cycles of 10 minutes during a measurement period of 90 hours. In order to perform a fair comparison we have configured each tool to work in the most favorable conditions. More specifically: 1) `rtl_test` runs during $\tau = 4$ minutes and averaging the cumulative frequency offset estimation every $\omega = 1$ minute; 2) `Kalibrate-RTL` executes taking as input the initial offset estimation as computed by `LTESS-track` in the previous time-bin; 3) `LTE-Cell-scanner` executes with default configuration (recall that the computation time is about 1 minute in the Raspberry-Pi). 4) `LTESS-track` is configured with an observation window of $W = 1$ second.

Fig. 9(a) shows the frequency offset estimates reported in each cycle of 10 minutes by the different tools for the non-TCXO "Blue" device. The first observation is that the frequency offsets in these devices are strongly depending on the temperature: the higher the temperature, the higher the instantaneous LO frequency, as can be seen more clearly in Fig. 9(c). `LTESS-track` and `LTE-Cell-Scanner` report very similar values except that the second one occasionally estimates the frequency offset with a large error. `Kalibrate-RTL` shows a similar trend of the frequency offset estimated but with a gap in the order of 1-2 ppm. Recall from Fig. 7 that the output values of this tool are somewhat dependent on the initial guess provided in input. It seems that the precision of this tool is somewhat limited to 1-2 ppm. By last, `rtl_test` reports very inaccurate frequency offset values even using the most favorable settings, with observation intervals of 4 minutes. Notice also that the resolution of the estimates provided by `rtl_test` is 1 ppm.

The long-term results for the TCXO "Silver" RTL-SDR device are shown in Fig. 9(b). The `rtl_test` tool again reports grossly inaccurate offset values (peaks of ± 10 ppm and average around -4 ppm), that the minimum resolution is 1 ppm. However the other 3 tools (`Kalibrate-RTL`, `LTE-Cell-Scanner` and `LTESS-track`) report similar values < 1 ppm. `Kalibrate-RTL` shows a higher gap compared to our method (0.5 ppm), but as said above, the precision of this tool is anyway coarser than 1 ppm. `LTE-Cell-Scanner` shows again occasional large errors (maximum peaks of -9 ppm). Besides those, we observe a small and systematic gap of 0.2 ppm between

the estimates delivered by `LTE-Cell-Scanner` and `LTESS-track` that could be caused by minor differences in the computation details between the two tools.

In Fig. 10(b), we plot the frequency offset of the TCXO RTL-SDR device as reported by `LTESS-track` versus the device temperature. The plotted data points span the whole measurement period of 90 hours. We can conclude that the stability of the TCXO device is well within the specifications (< 1 ppm). Notice that up to 50°C there is an approximately linear relation between frequency offset and temperature while in the range of $50\text{-}60^\circ\text{C}$ the frequency offset remains constant. On the other hand, non-TCXO RTL-SDR devices (Fig. 10(a)) shows an absolute frequency offset of several tens of ppm (50-70) with daily fluctuations around ± 5 ppm depending on the temperature. By last, Fig. 10(c) shows the linear relation between the temperature in the ambient and the temperature on the RTL-SDR device during operation. Both TCXO and non-TCXO devices seem to be 15°C above the temperature of the environment.

4.5 Computation performance

We have evaluated the execution time of every tool by measuring the time required to compute one single LO offset estimate. The tests are performed in a Quad-Core i5 laptop. `LTE-Cell-Scanner` reads samples for 160 ms and then computes a single frequency offset measurement in 15 seconds, due to the heavy computations needed for the PSS and SSS detection. However, `LTESS-track` is optimized for LO estimation and is able to provide a frequency offset measurement every second (reading samples for 0.5 seconds). `LTESS-track` is also 10 times faster than `Kalibrate-RTL` which performs each frequency offset measurement every 10 seconds. The evaluation of the `rtl_test` performance is not relevant since the performance depends on the the observation window, and the latter is 4 minutes long for this tool (besides the frequency offset estimated is not reliable).

5 CONCLUSIONS

We have introduced a precise and fast frequency offset estimator for low-cost SDR devices. `LTESS-track` exploits the synchronization signals broadcasted by LTE base stations to determine the LO offset of the RTL-SDR devices. `LTESS-track` implements several key mechanisms not presented in other methods such as initial frequency offset compensation, up-sampling, sampling of data only in time proximity to the expected synchronization signal to reduce the

computational cost and linear regression of samples. Our method is 10 times faster than the best open-source tools currently available, and is able to provide a new estimate every second. Therefore, our method allows to analyze and evaluate short-variations in time of the frequency offset. We have evaluated the two most common RTL-SDR devices in the market, the ones with TCXO integrated and the ones without. We have demonstrated that the frequency offset of the LO can be highly temperature dependent. Thanks to LTESS-track we can conclude that the maximum fluctuation in the TCXO "silver" device is around 0.2 ppm, while the non-TCXO "blue" device reports daily fluctuations of ± 5 ppm around an average value that can be in the order of 50-70 ppm. LTESS-track can be extended to work with any SDR front-end capable of tuning to LTE frequencies. The advantages of our approach become significant in crowd-sourced scenarios where LO frequency offsets need to be estimated quickly and compensated for a massive number of RTL-SDR devices deployed over a wide area. The MATLAB implementation of LTESS-track is released as open-source². We are currently working towards an optimized implementation in C/C++ designed to work with Raspberry-Pi.

REFERENCES

- [1] 2012. *kalibrate-rtl*. <https://github.com/steve-m/kalibrate-rtl>.
- [2] 2012. *LTE-Cell-Scanner*. <https://github.com/Evrytania/LTE-Cell-Scanner>.
- [3] 2016. *rtl_test*. https://github.com/steve-m/librtl_sdr.
- [4] 2016. *Silver v3 specifications*. <http://www rtl-sdr.com/buy-rtl-sdr-dvb-t-dongles/>.
- [5] Evolved Universal Terrestrial Radio Access. 2016. Physical channels and modulation. *3GPP TS 36.211* (2016). V8.
- [6] Ayon Chakraborty, Md Shaifur Rahman, Himanshu Gupta, and Samir R Das. 2017. SpecSense: Crowdensing for Efficient Querying of Spectrum Occupancy. In *IEEE INFOCOM*.
- [7] ETSI. 2013. *Evolved Universal Terrestrial Radio Access (E-UTRA); Base Station (BS) radio transmission and reception (3GPP TS 36.104)*.
- [8] Fred J. Harris. 2004. *Multirate Signal Processing for Communication Systems*.
- [9] S. Rajendran, R. Calvo-Palomino, M. Fuchs, B. Van den Bergh, H. Cordobés, D. Giustiniano, S. Pollin, and V. Lenders. 2017. Electrosense: Open and Big Spectrum Data. (2017). <https://arxiv.org/abs/1703.09989>
- [10] M. Schäfer, P. Leu, V. Lenders, and J. Schmitt. 2016. Secure Motion Verification using the Doppler Effect. *Proc. of the 9th ACM Conference on Security & Privacy in Wireless and Mobile Networks*.
- [11] S. Sesia. 2011. *LTE - The UMTS Long Term Evolution: From Theory to Practice*.
- [12] M. Strohmeier, M. Schäfer, M. Fuchs, V. Lenders, and I. Martinovic. 2015. OpenSky: A Swiss Army Knife for Air Traffic Security Research. In *Proceedings of the 34th IEEE/AIAA Digital Avionics Systems Conference (DASC)*.

²<https://github.com/electrosense/LTESS-track>